Journal of Biomolecular Structure & Dynamics, ISSN 0739-1102
Volume 7, Issue Number 6 (1990), ©Adenine Press (1990).

A Parallel Stranded Linear DNA Duplex Incorporating dG · dC Base Pairs

Karsten Rippe, Niels B. Ramsing†, Reinhard Klement and Thomas M. Jovin*
Max Planck Institute for Biophysical Chemistry
Department of Molecular Biology
P.O. Box 2841
D-3400 Göttingen, F.R.G.

Abstract

DNA oligonucleotides with appropriately designed complementary sequences can form a duplex in which the two strands are paired in a parallel orientation and not in the conventional antiparallel double helix of B-DNA. All parallel stranded (ps) molecules reported to date have consisted exclusively of dA · dT base pairs. We have substituted four dA · dT base pairs of a 25-nt parallel stranded linear duplex (ps-D1 · D2) with dG · dC base pairs. The two strands still adopt a duplex structure with the characteristic spectroscopic properties of the ps conformation but with a reduced thermodynamic stability. Thus, the melting temperature of the ps duplex with four dG · dC base pairs (ps-D5 · D6) is 10-16°C lower and the van't Hoff enthalpy difference ΔH_{vH} for the helix-coil transition is reduced by 20% (in NaCl) and 10% (in $MgCl_2$) compared to that of ps-D1 · D2. Based on energy minimizations of a ps-[$d(T_5GA_5)$ · $d(A_5CT_5)$] duplex using force field calculations we propose a model for the conformation of a *trans* dG · dC base pair in a ps helix.

Introduction

Pairs of deoxyoligonucleotides consisting of dA and dT sequences designed to be complementary only if the strands are oriented with the same polarity hybridize spontaneously into stable double-helical structures (1-6). Distinctive structural features of parallel stranded DNA (ps-DNA) derived from model calculations are *reverse* Watson-Crick base pairing with the glycosidic bonds in a trans orientation and the lack of distinct major and minor grooves. Parallel stranded duplexes exhibit spectroscopic, thermodynamic, and biochemical properties different from those of conventional antiparallel B-DNA, and are remarkably stable (1-6). For example, the enthalpy change associated with the helix-coil transition of ps-DNA is only 10-20% less than that of B-DNA (5,6), in qualitative agreement with the force field calculations of Pattabiraman who originally proposed the structure (7). All parallel

†Current address: Department of Ecology and Genetics, University of Århus, Ny Munkegade, DK-8000 Århus C, Denmark

*Author to whom correspondence should be addressed.

stranded (ps) molecules reported to date have consisted exclusively of dA · dT base pairs. The potential biological significance of this alternative helical structure, however, depends upon its feasibility in the case of natural sequences containing dG and dC as well. Therefore we have substituted four dA · dT base pairs of a parallel stranded linear duplex with dG · dC base pairs and compared its properties to that of the ps reference duplex consisting exclusively of dA · dT base pairs.

Materials and Methods

Oligonucleotide Synthesis and Characterization

The oligonucleotides were synthesized, purified, labelled with [^{32}P], and hybridized as described previously (4). The purity of the isolated end-labelled oligonucleotides was established by electrophoresis under denaturing conditions (4). No contaminating faster or slower migrating species could be detected (data not shown). Gel electrophoresis under native conditions was carried out in 14% polyacrylamide (5% crosslinking), 90 mM Tris-borate, pH 8.0, 2 mM $MgCl_2$ and at 20°C. The nuclease susceptibilities of ^{32}P-end labelled DNAs were assessed according to Ref. 8 with *Aspergillus oryzae S*1 nuclease (Pharmacia) and *Staphylococcus aureus (Micrococcal)* nuclease *S*7 (Sigma).

Spectroscopy

UV absorption measurements were made with a Uvikon 820 spectrophotometer equipped with computer-controlled thermostated cuvette holders and data acquisition (5) in 0.4 M NaCl and 10 mM Na-cacodylate, pH 7.1, unless otherwise indicated. The molar extinction coefficient of the oligonucleotides D1, D2, D3 and D4 was taken to be 8.6 mM (base)$^{-1}$ cm^{-1} at 264 nm in the denatured state (70 C standard buffer + 0.1 M NaCl; Figure 2B) (2,4). The corresponding extinction coefficients for D5 and for D6 in the denatured state were estimated by combining the dA · dT value cited above for D1-4 with the extinction coefficient for poly [d(G-C)] in the native (9) and denatured (Ramsing & Jovin, in preparation) state, and the corresponding value for denatured poly[dC] (10). We calculated an ε_{264} of 8.6 and 8.4 mmol base^{-1} cm^{-1} for D5 and D6, respectively, at 70°C. Circular dichroism (CD) spectra were acquired with a Jobin Yvon Model V Dichrograph in 2 mM $MgCl_2$, 10 mM Na-cacodylate, pH 7.1.

Model Force Field Calculations

Energy minimization was with the AMBER-PMF program (11) using 0.1 M NaCl as the supporting electrolyte in conjunction with the INSIGHT (Biosym Tech.) molecular modelling package and a PS390 Evans and Sutherland graphics workstation.

Results and Discussion

Design of Oligonucleotides

The set of 25-nt oligonucleotides D1, D2, D3 and D4 shown below were designed by

a computer aided search for complementary sequences capable of forming parallel stranded (ps) helices with minimal interference from competitive antiparallel (aps) secondary structures (4). The two ps-DNA duplexes, ps-D1 · D2, ps-D3 · D4, and the aps-D1 · D3 and aps-D2 · D4 references, were extensively characterized with respect to spectroscopic and thermodynamic properties (4-6) and were also tested as substrates for several DNA processing enzymes and chemical reagents (8). A comparison of the two combinations ps-D1 · D2 and ps-D3 · D4 with the corresponding aps molecules revealed the same characteristic differences found previously with other ps-DNA constructs (1-6).

In order to determine the influence of dG and dC residues on the properties of the parallel stranded helix, we synthesized two other 25-nt oligonucleotides designated as D5 and D6, in which four dA (D5) or four dT (D6) bases were replaced by dG and dC, respectively. Synthesis and purification were according to Ref. 4. The following combinations of the D1-D6 oligonucleotides were stable (see below):

Parallel stranded duplexes

```
D1: 5'-AAAAAAAAAATAATTTTAAATATTT-3'
      ••••••••••••••••••••••••••
    5'-TTTTTTTTTTATTAAAATTTATAAA-3' :D2

D3: 5'-AAATATTTAAAATTATTTTTTTTTT-3'
      ••••••••••••••••••••••••••
    5'-TTTATAAATTTTAATAAAAAAAAAA-3' :D4

D5: 5'-AAAAAGAAAGTAGTTTTAAGTATTT-3'
      ••••••••••••••••••••••••••
    5'-TTTTTCTTTCATCAAAATTCATAAA-3' :D6
```

Antiparallel stranded duplexes

```
D1: 5'-AAAAAAAAAATAATTTTAAATATTT-3'
      ••••••••••••••••••••••••••
    3'-TTTTTTTTTTATTAAAATTTATAAA-5' :D3

D2: 5'-TTTTTTTTTTATTAAAATTTATAAA-3'
      ••••••••••••••••••••••••••
    3'-AAAAAAAAAATAATTTTAAATATTT-5' :D4

D5: 5'-AAAAAGAAAGTAGTTTTAAGTATTT-3'
      ••••••••••••••••••••••••••
    3'-TTTTTTTTTTATTAAAATTTATAAA-5' :D3
```

Electrophoretic Properties

The generation and stability of the proposed duplex structures were assessed by gel electrophoresis under native conditions (2 mM $MgCl_2$, 20°C; Figure 1A). The only duplexes formed in addition to those described previously [ps-D1 · D2, ps-D3 · D4, aps-D1 · D3, aps-D2 · D4 (4,5)] corresponded to the combination D5+D6 (designated ps-D5 · D6) that has a sequence with four dG · dC base pairs and complementarity in a parallel orientation, and D5+D3 (antiparallel with four dG · dT mismatches). The other potential ps combinations involved either opposing dG and dT (D5+D2) or dA and dC (D1+D6) migrated in the position of single stranded species (with D1+D6 showing a slightly lower mobility).

Spectroscopic Properties

The ultraviolet absorption and circular dichroism spectra of the ps-D5 · D6 duplex are indicative of a base-paired structure resembling that of ps duplexes consisting only of dA · dT base pairs. Thus, both ps-D5 · D6 and ps-D1 · D2 show a characteristic blue shift in the native UV spectra relative to aps-D1 · D3 (Figure 2A), a feature particularly evident in the difference spectra (Figure 2B) and attributable to the dA · dT part of the sequence. Upon denaturation, the spectra (Figure 2B) demonstrate only the differences expected from the base composition. In Figure 2C the specific

dG · dC contribution in ps-D5 · D6 was calculated by subtracting the fractional dA · dT absorbance estimated from the spectra of ps-D1 · D2. In the denatured state, the specific dG · dC absorbance is similar to that of poly[d(G-C)] and to the estimated dG · dC contribution of poly d[(A-C) · d(G-T)]. In the native state, however, the calculated dG · dC spectrum of ps-D5 · D6 exhibits a higher absorbance, a general broadening, and a red shift of the peak compared to the reference DNAs. [As noted in the legend to Figure 2C, perturbations of the adjoining dA · dT base pairs may also contribute.]

The CD spectrum of ps-D5 · D6 compared to that of the aps-D1 · D3 reference in the native state (Figure 2D) shows the same features observed with ps-D1 · D2 above 265 nm (seen as a difference spectrum in Figure 2F) whereas at 250 nm the dichroism is reduced. The spectra in the denatured state are nearly similar for all three combinations (Figure 2E) showing only slight deviations attributable to the different base composition.

Helix-Coil Transition

Salt-dependent thermal transitions of various duplexes were monitored by the increase of UV absorption upon melting and represented as three-dimensional plots (Figure 3A-E). The absorbances at each temperature T and wavelength were normalized to the values at the initial (low) temperature T_0 in order to reveal the characteristic differences between the ps and aps conformation (2,4,5,6). The combination ps-D5 · D6 in $MgCl_2$ or NaCl displays the same distinctive hyperchromicity pattern found with ps-D1 · D2, ps-D3 · D4 and other ps DNAs (2,4,5,6). The melting temperature T_m of ps-D5 · D6 is 10-16°C lower than that of the corresponding duplex ps-D1 · D2 composed only of dA · dT base pairs and has the same salt dependence as the reference DNAs (Figure 3F, Table I). The van't Hoff enthalpy difference ΔH_{vH} for the helix-coil transition of ps-D5 · D6 is reduced by 20% (in NaCl) and 10% (in $MgCl_2$) compared to that of ps-D1 · D2, although it is greater than the value determined for a 21-nt ps duplex consisting exclusively of dA · dT base pairs (2,5,6). We calculated the mean dG · dC contribution per mole of nearest neighbors (N.N.) of ps-D5 · D6, $\Delta h_{dG \cdot dC}$, by assuming that the substitution of the 4 dG · dC base pairs out of 25 leads to a change in 8 N.N. interactions. The resulting expression ($\Delta h_{dG \cdot dC} = [\Delta H_{ps\text{-}D5 \cdot D6} - 16/24 \cdot \Delta H_{ps\text{-}D1 \cdot D2}]/8$) yields 8 kJ · mol^{-1} in NaCl and 14 kJ · mol^{-1} in $MgCl_2$, respectively, and can be compared to the mean values for the

---

Legend for Color Folio

Figure 4: Model of dG · dC base pair in ps[d(T_5GA_5) · d(A_5CT_5)] optimized by force field calculations. (A) Side-view of the central three base pairs; 5′ ends are at the bottom. (B) Cros-sectional view of the central dG · dC (ball and stick) and underlying dA · dT (space filling) base pair. Color coding: sugars, white; phosphates (including O3′ and O5′), red; adenine, cyan; thymine, yellow; thymine methyl groups, turquoise; guanine, blue; cytosine, green. The figure was generated by the SCHAKAL v86b program of Dr. E. Keller, Univ. of Freiburg, FRG. The model was generated by extracting the 3′ terminal 11 residues from an optimized 21-nt ps duplex (2) and refining the resultant 11-nt ps-[d(T_5A_6) · d(A_5T_6)] duplex as well as the sequence in which the central dA · dT base pair was replaced by dG · dC.

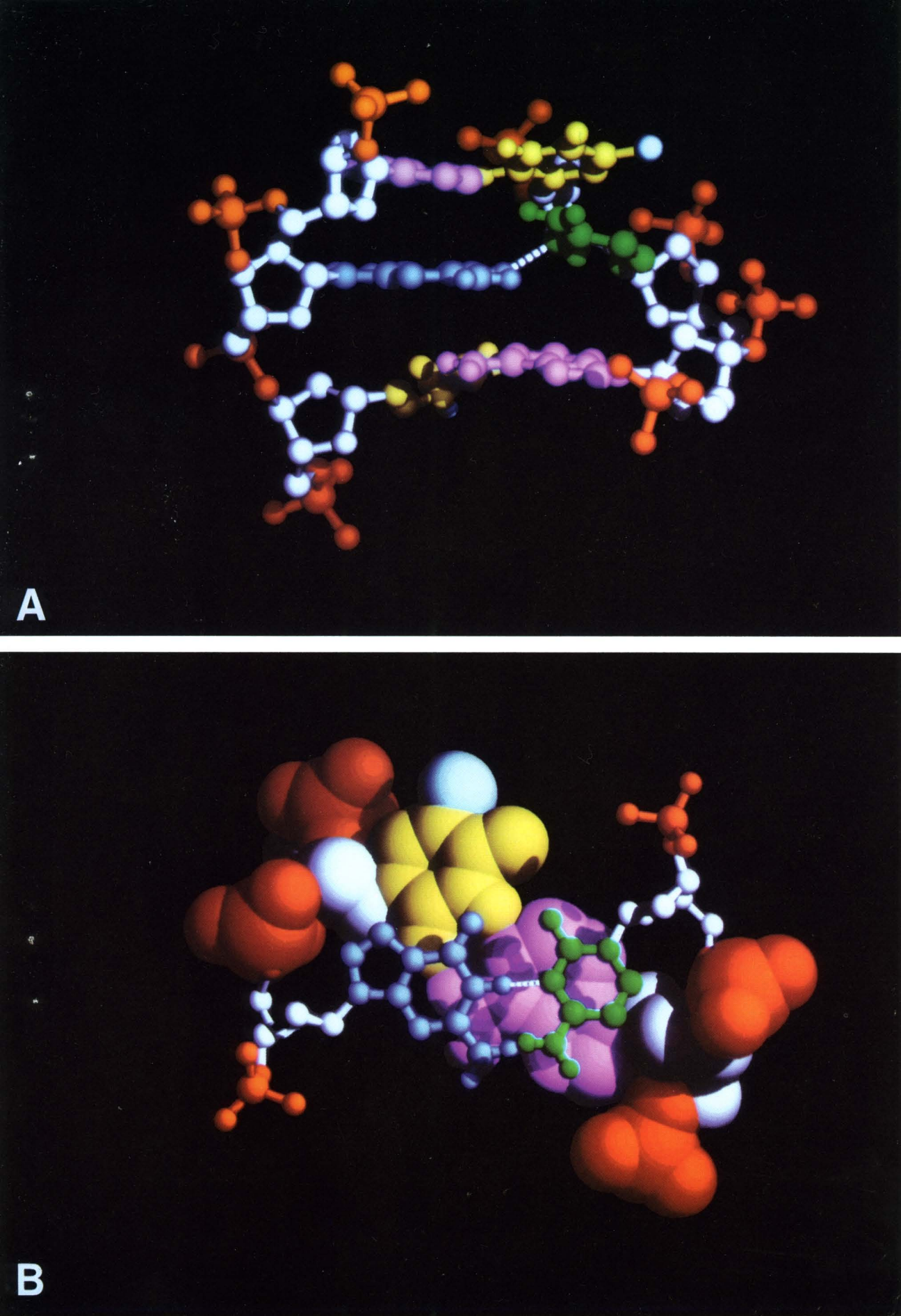
A
B

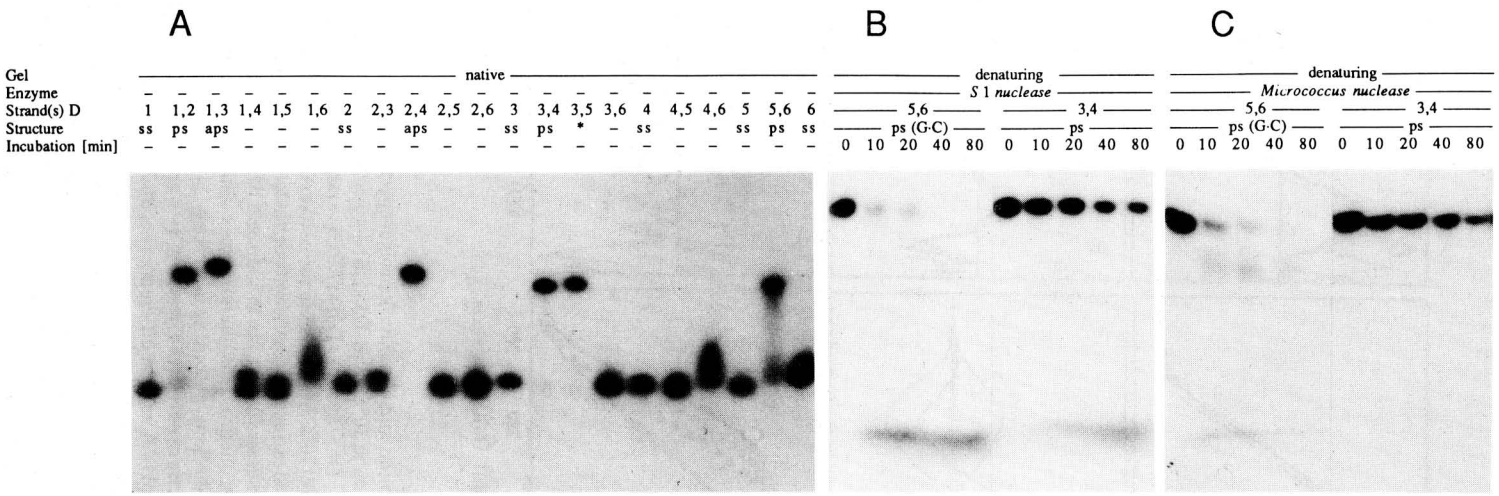

Figure 1: Electrophoretic analysis of duplex formation and of degradation by *S*1 and *S*7 nuclease activities. (A) Native polyacrylamide gel at 20°C of the different combinations of labelled D1, D2, D3, D4, D5 and D6, aps with wobble G-T base pair. (B) Digest of ps-D5 · D6 and ps-D3 · D4 (all strands labelled) at 10°C with *S*1 nuclease. (C) Digest of ps-D5 · D6 and ps-D3 · D4 (all strands labelled) at 10°C with *S*7 nuclease.

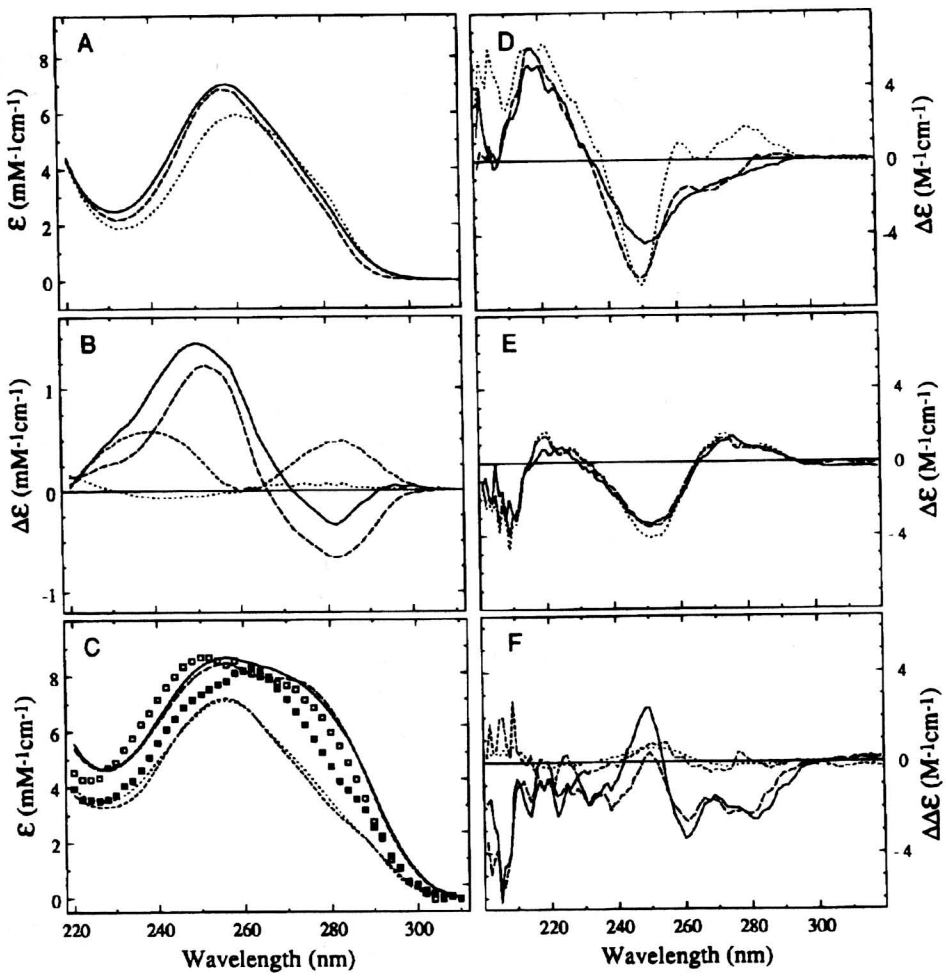

Figure 2: Ultraviolet absorption and circular dichroism spectra of ps and aps oligonucleotides. (A-C) UV-spectra. (A) Native spectra at 10°C of ps-D5 · D6 (—), ps-D1 · D2 (– – –) and aps-D1 · D3 (·····). (B) Difference spectra of [ps-D5 · D6 – aps-D1 · D3] at 10°C (—) and at 70°C (-----) and of [ps-D1 · D2 – aps-D1 · D3] at 10°C (– – –) and at 70°C (·····). (C) ε^* in the native state at 10°C (■) and in the denatured state at 70°C (□). ε^* is the calculated extinction coefficient per nucleotide for a dG · dC base pair in ps-D5 · D6, including possible spectral changes ($\Delta\varepsilon_{dA \cdot dT}$) in the adjacent dA · dT residues compared to the equivalent positions in the ps-D1 · D2 sequence. This quantity was estimated by assuming additivity of unit contributions and negligible end effects, according to $\varepsilon^* = \varepsilon_{dG \cdot dC} + 2\Delta\varepsilon_{dA \cdot dT} = 25/4 \cdot (\varepsilon_{ps\text{-}D5 \cdot D6} - 21/25 \cdot \varepsilon_{ps\text{-}D1 \cdot D2})$. As references, the spectra of poly[d(G-C)] at 10°C (·····) and at 70°C (– – –) in 0.2 mM Tris-HCl, 0.2 mM NaCl, 0.02 mM EDTA, pH 7.0, and the difference spectra 2 · poly[d(A-C) · d(G-T)] – aps-D1 · D3 at 10°C (-----) and at 70°C (—) in 1 mM Tris-HCl, 1 mM NaCl, 0.1 mM EDTA, pH 7.0, are shown. The ε_{260} of poly[d(A-C) · d(G-T)] was 6.5 mM (base)$^{-1}$ cm^{-1} at 25°C (15). (D-F) Circular dichroism (CD) spectra. (D) Native spectra at 10°C: ps-D5 · D6 (—), ps-D1 · D2 (– – –) and aps-D1 · D3 (·····). (E) Melted duplexes at 70°C, same symbols as before. (F) Difference spectra at 10°C: ps-D5 · D6 – aps-D1 · D3 (—), ps-D1 · D2 – aps-D1 · D3 (– – –); at 70°C: ps-D5 · D6 – aps-D1 · D3 (-----), ps-D1 · D2 – aps-D1 · D3 (·····).

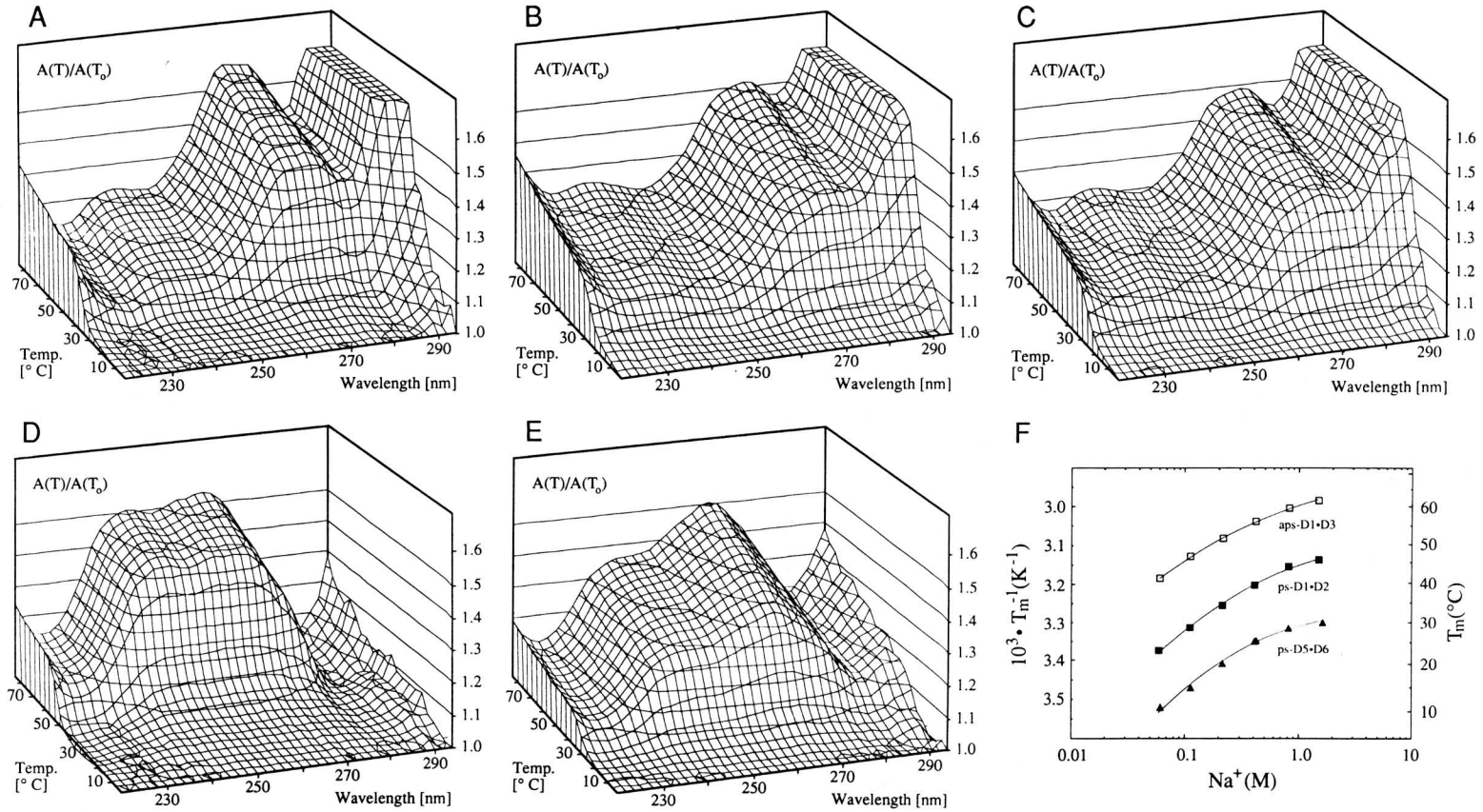

Figure 3: Thermally-resolved ultraviolet absorption spectra of ps and aps helices and salt dependence of melting temperature. (A-E) Hyperchromicity expressed as the absorbance ratio, $A_\lambda(T)/A_\lambda(T_o)$, where T_o is the initial temperature. All spectra were taken in 10 mM Na-cacodylate, pH 7.1, and in 2 mM $MgCl_2$, if not otherwise noted. (A) ps-D1 · D2. (B) ps-D5 · D6. (C) ps-D5 · D6 in 0.4 M NaCl. (D) aps-D1 · D3. (E) aps-D3 · D5, an antiparallel duplex with 4 dG · dT mismatches. Such wobble base pairs (involving hydrogen bonding between O6 and HN1 of guanine with HN3 and O2 of thymine) can be accommodated in the B-DNA helix with minimal perturbation of the structure (16,17). The aps-D3 · D5 has a T_m of 29.9°C in 2 mM $MgCl_2$ and a ΔH_{vH} of 442 kJ/mol. The change per dA · dT to dG · dT substitution of 74 kJ/mol is in agreement with the results of another study (16). (F) Melting temperature of ps-D5 · D6 (▲), ps-D1 · D2 (■), and aps-D1 · D3 (□) as a function of salt concentration. The solid lines are a second order regression. The UV spectra were recorded in steps of 2 nm from 220-320 nm at 4° intervals in the range 2-96°C for both heating and cooling cycles. The data sets were acquired, corrected, analyzed, and plotted as described elsewhere (5). T_m values were determined from the absorbance values obtained from the initial heating cycle of the thermal melting profile and corrected to a DNA concentration of 1.6 μM strands according to Ref. 5.

Table I
Thermodynamic Parameters for Helix-Coil Transition or ps and aps Duplexes

Duplex	Salt	T_m[a] °C	ΔH_{vH} kJ · mol^{-1}	ΔS kJ · mol^{-1}K^{-1}	ΔG kJ · mol^{-1}	Δh kJ · mol^{-1}	Δs J · mol^{-1}K^{-1}	Δg kJ · mol^{-1}
			Total			per N.N.[b]		
ps-D5 · D6	NaCl	15.7	372	1.17	24	16	49	1.0
	$MgCl_2$	25.3	451	1.39	37	19	58	1.5
ps-D1 · D2	NaCl	29.0	459	1.40	42	19	58	1.7
	$MgCl_2$	35.7	507	1.52	53	21	63	2.2
aps-D1 · D3	NaCl	46.4	670	1.97	80	28	82	3.3
	$MgCl_2$	50.8	736	2.15	94	31	90	3.9

Thermodynamic values for the helix-coil transition. The data from experiments under various ionic conditions were compatible with an all-or-none two state model for the transition (5). The measurements were made in 10 mM Na-cacodylate, pH 7.1, and 0.05-1.6 M NaCl (see also Figure 3F) or 0.12-8 mM $MgCl_2$. DNA concentrations are scaled to a total strand concentration of 1.6 μM (5). The listed values are averages, the 95% confidence limits of which were < 5% of the means (see Refs. 4,5). The van't Hoff enthalpy differences for the helix-coil transition were calculated from data in the range of 0.1-1 M NaCl and 0.5-8 mM $MgCl_2$. ΔS and ΔG were determined according to Refs. 5 and 6 and correspond to T_m and 25°C, respectively.
[a] T_m in 0.1 M NaCl and 2 mM $MgCl_2$, respectively; calculated from regression lines as in Figure 3F.
[b] Total values divided per nearest neighbor interactions (N.N.), n − 1 = 24.

entire molecule and for ps-D1 · D2 (Table I). We conclude that the dG · dC base pair provides a positive enthalpic contribution to the helical stability of ps DNA that is about half (0.4 in NaCl, 0.7 in $MgCl_2$) of the dA · dT base pair. A complete thermodynamic analysis (4,5) yields the entropic and free energy terms for the helix-coil transition (Table I). The T_m of ps-D5 · D6 in 2 mM $MgCl_2$ and at a total strand concentration of 10 μM is 28°C; at 20°C, 95% of the DNA would be in the duplex form.

Substrate Specificities

The ps-D5 · D6 duplex was tested as a substrate for the single strand specific *S*1 and *S*7 nucleases (Figure 1b, 1c) (8). The rate of degradation of ps-D5 · D6 was higher than that of ps-D3 · D4 (with only dA · dT base pairs) in the case of both enzymes. In addition, preferred cutting sites appeared with *S*7 nuclease. These effects may derive from the reduced thermodynamic stability of ps-D5 · D6 as well as from an altered exposure of the sugar-phosphate backbone at the locus of the dG · dC base pairs.

Base Pairing and Model Structure

Base pairing between dG and dC in a helix with parallel orientation of the constituent strands leads to the loss of at least one hydrogen bond compared to a normal *cis*-Watson-Crick base pair unless compensatory tautomerizations occur. The dG · dC base pair in a *trans* conformation, referred to here as a *trans*-Crick-Watson (*trans*-CW) dG · dC base pair is found as the RNA equivalent in yeast $tRNA^{phe}$ between G15 (dihydrouridine loop) and C48 (variable loop) (12). It stabilizes the tertiary

structure of the molecule by stacking and two hydrogen bonds between HN1 and HN2 of guanine and O2 and N3 of cytosine in a segment with a parallel chain orientation. The corresponding interaction in yeast $tRNA^{asp}$ is mediated by a *trans*-CW $A_{15} \cdot U_{48}$ base pair (13).

The dG · dC base pair in ps-DNA was modeled by minimizing the energy of a ps-[$d(T_5GA_5) \cdot d(A_5CT_5)$] duplex using force field calculations. A comparative analysis (not shown) was also carried out of the corresponding aps structure and of the parent ps-[$d(T_5A_6) \cdot d(A_5T_6)$] and aps-[$d(T_5A_6) \cdot d(T_6A_5)$] duplexes. The final helical conformation is depicted in Figure 4A as a side-view of the central three base pairs and in Figure 4B as a cross-sectional overlay of the dG · dC base pair and the underlying dA · dT base pair. The following average features of the optimized ps-[$d(T_5GA_5) \cdot d(A_5CT_5)$] duplex were derived from the central 7 residues (see Ref. 14 for nomenclature). (i) All nucleotides have an *anti* ($<\chi> = -111°$) conformation of the glycosidic bond and a C2'-*endo* sugar pucker. [We were unable to generate an

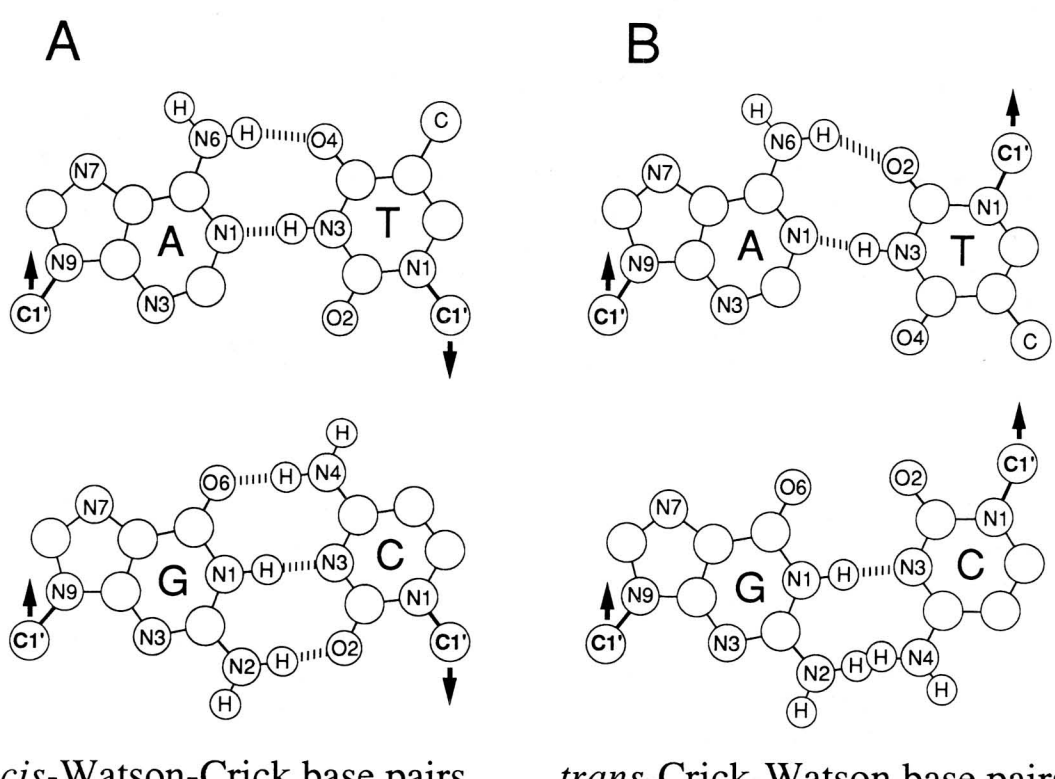

Figure 5: Base pairs in aps and in ps DNA. (A) dA · dT and dG · dC *cis*-Watson-Crick base pairs derived from positions A5-B8 and A9-B4 in the Drew-Dickerson B-DNA dodecanucleotide (entry 1BNA in the Brookhaven Protein Data Bank). (B) dA · dT and dG · dC *trans*-Crick-Watson base pairs from positions 4 and 6 of the minimized ps-[$d(T_5GA_5) \cdot d(A_5CT_5)$] duplex. The purine bases have been constrained to lie in the plane of the drawing so that the pyrimidines appear in projection.

alternative helical structure for the given sequence incorporating combinations of *anti* (pyrimidine) and *syn* (purine) glycosidic conformations.] (ii) The two glycosidic bonds of each base pair are in a *trans* conformation with the sugar-phosphate chains oriented parallel to each other. The base pairs show significant propeller twist (−25°), buckle (up to a magnitude of 33°), and shear (25°). (iii) The mean helical twist is 42° and helical rise 3.1°, a value ~15% greater than that calculated for the corresponding aps duplex. From a comparison with ps-[d(T_5A_6) · d(A_5T_6)], we conclude that the introduction of dG · dC does not lead to major perturbations of the helix inasmuch as the flanking segments in the optimized structure of both duplexes were superimposable.

An interesting finding from the above analysis is that the *trans*-CW dA · dT and dG · dC base pairs are more nearly isomorphous than one would have anticipated. Thus, from the minimized structures we derive C1′-C1′ distances of 10.7 Å (dA · dT) and 11.0 Å (dG · dC), and the C1′-N angles are 35, 46, 28, and 44° for the A, T, C, and G bonds, respectively. We propose in Figure 5B a set of *trans*-CW dA · dT and dG · dC base pair structures as representative for ps-DNA. The canonical *cis*-WC structures are depicted by way of comparison (Figure 5A).

A single hydrogen bond (between HN1 of G and N3 of C) is shown for the *trans*-CW dG · dC base pair corresponding to a distance in the refined structure of 2.9 Å. This result was independent of the chosen starting structure including one with two H-bonds as found in yeast $tRNA^{phe}$. We note that the restrictions imposed by the backbone of the ps-[d(T_5GA_5) · d(A_5CT_5)] duplex are not shared by the single *trans*-CW dG · dC base pair in tRNA. The other potential *trans*-CW base pairing combinations in ps-DNA (dG · dT in D5+D2, dA · dC in D1+D6; see Figure 1A) are apparently less stable than dG · dC. This might be due to the fact that the observed propeller twist in the *trans*-CW base pairs would weaken the potential H-bonds in the dG · dT (between HN2 of G and O4 of T) and dA · dC (between HN6 of A and O2 of C) base pairs, by increasing the distances between donor and acceptor.

Concluding Remarks

The finding that the ps conformation can accommodate both dA · dT and dG · dC base pairs increases the potential for this structure in the mediation of secondary and tertiary interactions in DNA, and, possibly, RNA. We have previously identified sequence relationships which would facilitate the formation of ps helical regions (2). The establishment of their occurrence will require direct analysis of natural sequences, further physicochemical studies of model duplexes particularly by crystallographic and NMR techniques, and a concerted search for specific recognition proteins.

Acknowledgments

We thank Gudrun Heim for valuable technical assistance.

References and Footnotes

1. van de Sande, J.H., Ramsing, N.B., Germann, M.W., Elhorst, W., Kalisch, B.W., v. Kitzing, E., Pon, R.T., Clegg, R.M. and Jovin, T.M., *Science 241*, 551-557 (1988).

2. Ramsing, N.B. and Jovin, T.M., *Nucleic Acids Res. 16*, 6659-6676 (1988).
3. Germann, M.W., Kalish B.W. and van de Sande, J.H., *Biochemistry 27*, 8302-8306 (1988).
4. Rippe, K., Ramsing, N.B. and Jovin, T.M., *Biochemistry 28*, 9536-9541 (1989).
5. Ramsing, N.B., Rippe, K. and Jovin, T.M., *Biochemistry 28*, 9528-9535 (1989).
6. Jovin, T.M, Rippe, K., Ramsing, N.B., Klement, R., Elhorst, W., and Vojtišková, M., *Structure & Methods, Vol. 3: DNA & RNA*, Eds., Sarma, R.H. and Sarma, M.H., Adenine Press, Schenectady, NY, 155-174 (1990).
7. Pattabiraman, N., *Biopolymers 25*, 1603-1606 (1986).
8. Rippe, K. and Jovin, T.M., *Biochemistry 28*, 9542-9549 (1989).
9. Pohl, F.M. and Jovin, T.M., *J. Mol. Biol. 67*, 375-396 (1972).
10. Inman, R., *J. Mol. Biol. 9*, 624-637 (1964).
11. Klement, R., Soumpasis, D.M., v. Kitzing, E. and Jovin, T.M., *Biopolymers*, in press (1990).
12. Kim, S.H., Sussman, J.L., Suddath, F.L., Quigley, G.J., McPherson, A., Wang, A.H.J., Seeman, N.C. and Rich, A., *Proc. Natl. Acad. Sci. USA 71*, 4970-4974 (1974).
13. Westhof, E., Dumas, P. and Moras, D., *J. Mol . Biol. 184*, 119-145 (1985).
14. Saenger, W., in *Principles of Nucleic Acid Structure*, Springer-Verlag, New York, (1984) [see also *EMBO J. 8*, 1-4 (1989)].
15. Wells, R.D., Larson, J.E. and Grant, R.C., *J. Mol. Biol. 54*, 465-497 (1970).
16. Brown, T., Kennard, O.J., Kneale, G. and Rabinovich, D., *Nature 315*, 604-606 (1985).
17. Aboud-ela, F., Koh, D. and Tinoco Jr., I., *Nucleic Acids Res. 13*, 4811-4824 (1985).

Date Received: January 1990

Communicated by the Editor David Lilley